THE JOURNAL OF PHYSICAL CHEMISTRY B

ARTICLE

pubs.acs.org/JPCB

Structural Examination of the Impact of Glycerol on Water Structure

J. J. Towey and L. Dougan*

School of Physics and Astronomy, University of Leeds, Leeds, LS2 9JT, United Kingdom

ABSTRACT: The sugar alcohol glycerol is essential for cryopreservation, an important process used for the storage of biological molecules, cells, or tissues at low temperatures. A key hypothesis for the cryoprotective action of glycerol is that the glycerol molecule acts to modify the hydrogen bonding ability of water molecules, thus inhibiting ice formation. In this study, high-resolution neutron diffraction has been used in conjunction with hydrogen/deuterium isotopic labeling to determine with unprecedented detail the structure of a dilute aqueous glycerol solution. Contrary to some expectations, at the first neighbor level no modification in the position of the coordination shell of water is observed. However, at the second neighbor level the presence of only small quantities of glycerol in the solution has the same impact on water structure as increasing the pressure. Evidence is also found of more glycerol monomers than would be expected in the solution. This prevalence of isolated glycerol molecules results in a very well mixed solution with glycerol−water hydrogen bond interactions being very favorable. Our results indicate that while the local structure of water is relatively unperturbed by the presence of glycerol, the hydrogen bonded network is highly mixed between glycerol and water. These results indicate that efforts to explain the action of glycerol should focus on not just local water structure, but the extended hydrogen bonded network in the system.

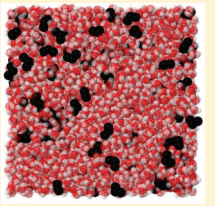

1. INTRODUCTION

Glycerol ($CH_2OHCHOHCH_2OH$) is a sugar alcohol with three hydroxyl groups that are thought to be responsible for its high solubility in water (Figure 1). Liquid glycerol exhibits an anomalous temperature behavior of the viscosity coefficient[1,2] and of dielectric relaxation times,[3,4] thought to be due to the existence of an extended hydrogen-bond network.[5] On account of molecular flexibility, asymmetry and ability to form hydrogen bonds, glycerol is an intricate substance to study at the molecular level. Aqueous mixtures of glycerol are used to preserve the functionality of biological molecules during cooling and thawing processes, and to suppress intracellular ice formation, which can be harmful to cells and tissues.[6−8] While vital for many processes, the molecular mechanisms by which cryoprotectants stabilize and protect molecules and cells, along with suppressing the formation of ice, are incompletely understood. Elucidating such molecular mechanisms is crucial to improve cryopreservation protocols as well as to identify and formulate more efficient cryoprotectant solutions.[9] As well as their importance in the storage of biological molecules in industry and medicine, cryoprotectants are prevalent in nature in a wide range of organisms.[10] Glycerol is a common cellular component and exists in algae, salt-tolerant plants, insects, fish, and reptiles that are exposed to cold temperatures. In these organisms glycerol is used as a colligate cryoprotectant that is thought to raise the osmolarity of body fluids and reduce the water available to form extracellular ice.[11] For example, glycerol acts as an effective cryoprotectant in the blood of some insects, rising in concentration in the larvae of the parasitic wasp *Bracon cephi* before the onset of winter, and falling again in spring.[12] While the occurrence of glycerol in nature has long been noted, elucidating the molecular mechanisms by which glycerol molecules influence the stability of biological molecules has proven to be challenging.[10,13]

To understand how glycerol functions as a glass former and cryoprotectant, the physical properties of glycerol and its mixtures with water have been studied extensively using a number of methods including molecular dynamics,[14−19] thermodynamic measurements,[20] NMR,[14,21] infrared,[22] and Raman spectroscopy.[21−23] While these studies have provided useful insights for understanding the dynamic behavior of glycerol, the manner in which glycerol hydrogen bonds is yet to be fully understood. Indeed, a correspondingly thorough understanding of the structure of glycerol, at the molecular level, could help to explain the behavior of a broad family of other glass formers. Given the importance and extensive use of glycerol, it is perhaps surprising that the current understanding of its fundamental liquid structure is almost exclusively derived from computer simulations. All these investigations have been parametrized to reproduce some macroscopic physical properties, such as the liquid's diffusion coefficient, but they are entirely dependent upon on the resulting interatomic and intermolecular force fields for the reproduction of structural parameters. Due to the absence of any parametrization to data that is directly related to atomic and molecular structure, conclusions derived from these models concerning local structure remain inconclusive. One fundamental and recurring hypothesis is that cryoprotectants such as glycerol act by modifying water structure, thus altering the ice-forming ability of water. A previous molecular dynamics simulation study of hydrogen bonding in dilute aqueous glycerol solutions (0.031−0.133 mole fraction (m.f.) glycerol)[18] suggested that glycerol molecules act to decrease the hydrogen bonding "ability" of water molecules. In another molecular dynamics simulation study, a range of polyols (including glycerol) were studied at dilute concentrations (0.06 m.f.),[24] and it was found that the tetrahedral hydrogen bonding network of water is diminished upon polyol solvation, and water forms

Received: September 28, 2011
Revised: November 25, 2011
Published: November 29, 2011

dx.doi.org/10.1021/jp2093862 | *J. Phys. Chem. B* 2012, 116, 1633–1641

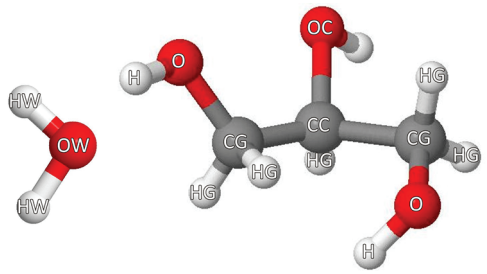

Figure 1. The glycerol and water molecules. Atoms have been labeled according to the symbols used in the simulation and throughout this paper. For glycerol, the carbon atoms are labeled CG and CC, the oxygen atoms O and OC, the hydroxyl hydrogen atoms H, and the methyl hydrogen atoms HG. The water oxygen is labeled OW and the water hydrogen HW.

weaker hydrogen bonds with the solute molecules than with other water molecules. Conversely, a study using fundamental thermodynamic relations, found no correlation between a cryoprotectants impact on water structure and its ability to stabilize a biological molecule.[25] Instead, the study suggested that efforts to explain cryoprotectant actions should focus on other hypotheses, including those based on preferential interactions and excluded volume effects. Raman spectroscopy studies of glycerol/D_2O solutions at dilute glycerol concentrations (0.02, 0.12, and 0.32 m.f. glycerol)[23] suggested that D_2O preferentially bonds to the central oxygen of glycerol at these concentrations. In addition, glycerol−glycerol bonds were found to break when the concentration is lowered to 0.02 m.f., leading to an increase in the proportion of monomeric glycerol molecules. Koga et al. have reported measurements of the thermodynamic properties of aqueous glycerol[20] from which they derive information on the molecular-scale mixing of the solutions. In this study, below ∼0.1 m.f. the water molecules act similarly to bulk water, while between ∼0.1 and ∼0.35 m.f. water/glycerol molecules segregate into regions of relatively high water/glycerol concentration.

The variability of results produced using computer simulations mean that a more direct experimental probe of liquid structure is required to determine the influence of glycerol on the local and extended water structure. Over the past decade, significant advances have been made in the methods of neutron diffraction with isotopic substitution and in the development of more powerful computational tools for inverting the resulting experimental data to a three-dimensional structural model.[26−28] Consequently, it is now possible to experimentally establish the structure of this important cryoprotectant system. In this paper, a combination of high-resolution neutron diffraction and isotopic substitution of hydrogen for deuterium has been used to determine the detailed structure of a dilute glycerol solution (0.05 m.f. glycerol). Data analysis using the empirical potential structure refinement method (EPSR) has allowed us to obtain a full three-dimensional spatial picture of the liquids and thereby to answer key questions and test specific hypotheses concerning the hydrogen bonding ability of glycerol and water. This structural approach provides the first detailed experimental insight into this system and allows a number of previous models to be tested for the first time.

2. METHODS

2.1. Neutron Diffraction Experiments. Neutron diffraction experiments were completed on the small angle neutron diffractometer for amorphous and liquid samples (SANDALS) time-of-flight diffractometer at the ISIS pulsed neutron facility within the Rutherford Appleton Laboratory, UK. This instrument is optimized for the study of liquids containing light elements and, in particular, for hydrogen/deuterium isotopic substitution techniques, taking full advantage of the very large difference in neutron scattering lengths between hydrogen (b_H = −3.74 fm) and deuterium (b_D = 6.67 fm).[29] To facilitate the direct extraction of the intermolecular structural correlations between glycerol and water molecules, five samples were measured (Table 1). Deuteriated samples of water along with protiated and deuterated samples of anhydrous glycerol were obtained from Sigma-Aldrich and used without additional purification. All samples were placed in flat cells made from a titanium−zirconium alloy which gives negligible coherent scattering signal.[29] These cells were mounted on an automated sample changer to cycle through the samples. During measurement, the cell was maintained at the ambient temperature of the instrument 25 °C. The scattering data were collected over scattering angles (2θ) between 3° and 40° and analyzed using neutron wavelengths in the range λ = 0.075−3.5 Å over a corresponding Q-range for each data set ranging from 0.1 to 30 $Å^{-1}$. After collection, the data were analyzed using the Gudrun routines that are based upon basic algorithms in the widely used ATLAS package.[30] These routines correct the data for contributions from the empty cell, instrument background, absorption, and multiple scattering and normalize the data to absolute units using the scattering of a vanadium standard. The remaining corrections to account for the contributions from inelastic scattering by the sample were made using the methods outlined by Soper.[31]

2.2. Theory. Following corrections, the function extracted from a neutron diffraction experiment is the total structure factor $F(Q)$, which is defined in terms of the magnitude of the scattering vector Q

$$Q = \frac{4\pi}{\lambda}\sin\theta \tag{1}$$

where λ is the wavelength of the incident neutrons, and 2θ is the scattering angle.[29] The total structure factor can then be written as

$$F(Q) = \sum_{\alpha \le \beta} (2 - \delta_{\alpha\beta}) c_\alpha c_\beta b_\alpha b_\beta (S_{\alpha\beta}(Q) - 1) \tag{2}$$

The structure factor contains information relating to the pairwise spatial correlations between atoms of type α and β, reflected in the sum over the partial structure factors, $S_{\alpha\beta}(Q)$. These terms are weighted by the respective concentrations, c_α and c_β, and the scattering lengths b_α and b_β, of each atom type. The Kronecker delta function $\delta_{\alpha\beta}$, is used to prevent double counting of like terms within the summation.[29] The structure factors, either composite or partial, can be inverted to real space atomic pair distribution function, $g_{\alpha\beta}(r)$, by a Fourier transform weighted by the atomic density, ρ:

$$(S_{\alpha\beta}(Q) - 1) = 4\pi\rho \int_0^\infty r^2 (g_{\alpha\beta}(r) - 1) \frac{\sin Qr}{Qr}\, dr \tag{3}$$

$g_{\alpha\beta}(r)$ represents the real space correlations between pairs of atoms as a function of their separation, r, and is the primary aim of most structural studies of liquids. In addition to the interatomic distance information, integrating this function over a range in r allows us to access the number of atoms of type β that would be

Table 1. Glycerol−Water Samples for Which the Structure Factor Has Been Measured with Neutron Diffraction on the SANDALS Instrument[a]

sample no.	sample name	description
1	glycerol-D_8 D_2O	fully deuterated glycerol (98 atom % D) with D_2O (99.99 atom % D)
2	glycerol-D_5 H_2O	carbonyl atoms are deuterium and hydroxyl are hydrogen (98 atom % D) with Milli-Q water
3	glycerol-D_5HD_3 HDO	1:1 mixture of samples 1 and 2 with a 1:1 mixture of Milli-Q water and D_2O (99.99 atom % D)
4	glycerol-H_8 H_2O	fully protiated glycerol (99.5%) with Milli-Q water
5	glycerol-HD_8 HDO	1:1 mixture of samples 1 and 4 with a 1:1 mixture of Milli-Q water and D_2O (99.99 atom % D)

[a] Deuterium oxide D_2O (99.5%), glycerol (99.5%), glycerol-d_3 (98 atom % D), and glycerol-d_8 (98 atom % D) were supplied by Sigma-Aldrich.

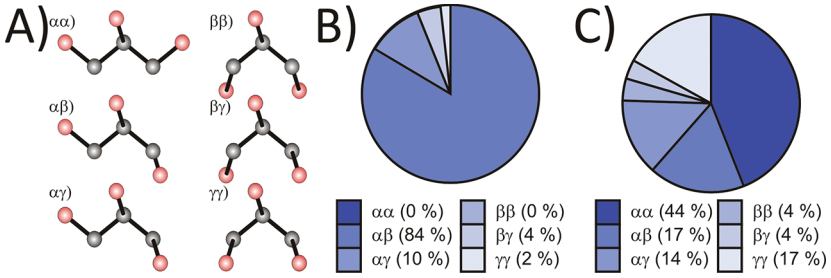

Figure 2. (A) A schematic diagram of the six conformers of glycerol as defined by Bastiensen.[16] Here, the oxygen atoms are red and the carbon atoms are black. The hydrogen atoms have been removed to aid clarity. (B) The conformational distribution of glycerol molecules in a pure glycerol liquid at 298 K.[36] (C) The distribution of glycerol molecules conformers in a dilute glycerol−water mixture (0.05 mol fraction glycerol) at 298 K.

found around an atom of type α within the specified range. This is known as the coordination number, $n_{\alpha\beta}$, and is the average number of atoms of type β that are within a defined distance of a central atom, α. This is expressed as

$$n_{\alpha\beta} = 4\pi\rho c_\beta \int_{r_{min}}^{r_{max}} r^2 g_{\alpha\beta}(r)\, dr \qquad (4)$$

where $n_{\alpha\beta}$ is the average number of atoms of type β around each atom of type α, ρ is the density of the system (atoms Å^{-3}), and c_β is the number fraction of atom β.

2.3. Computational Modeling. In this study, the technique of EPSR has been used to build a three-dimensional model of the structure of the liquid that is consistent with the five measured total structure factors.[32] In this paper we refer to two distinct atomic components in water and six distinct atomic components in glycerol molecules (see Figure 1). In the water molecule, the oxygen atom is labeled OW, while the hydrogen atom is labeled HW. In glycerol, the carbon atoms are labeled CC and CG and refer to the central and distal carbon atoms, respectively. The oxygen atoms are labeled OC and O corresponding to the oxygen atoms attached to the central and distal carbon atoms, respectively. The hydrogen atoms are labeled H and HG for the hydroxyl and methyl hydrogen atoms, respectively. A full structural characterization of the system requires the determination of 36 radial distribution functions (RDFs), which is well beyond the capability of any existing diffraction techniques by themselves.

To build a model of glycerol and water liquid structure, the experimental data are used to constrain a computer simulation. In the EPSR simulation, the empirical potential is obtained directly from the diffraction data. This potential drives the structure of the three-dimensional model toward molecular configurations that are consistent with the measured partial structure factors from the neutron diffraction experiments. EPSR aims to produce a model with simulated partial structure factors that fit the experimental results as closely as possible.[33] Given that in this case there are more site−site RDFs than diffraction data sets, extra information is required to define the structure. This is achieved by forcing the glycerol molecules in the simulation box to adopt the expected molecular geometries. A reference interaction potential is used which serves to generate hydrogen bonding between the relevant atom sites and to prevent atomic overlap at unrealistic distance ranges. The combined empirical and reference potentials do not guarantee the final reconstruction of the structure is unique, but they do ensure that it is consistent with the diffraction data as well as being physically plausible.

For the simulations, a total of 200 glycerol molecules and 3800 water molecules were contained in a cubic box of the appropriate dimension to give the measured density at 298 K. The intramolecular structure was optimized using the computational chemistry software Ghemical 2.98.[34] The optimization procedure consists of 500 steps using a conjugate gradient algorithm and the atomic potentials provided as part of the software package. The intramolecular bond angles were defined using the conformer definitions of Bastiensen,[35] according to the dihedral angles involving the two CCCO torsions. Each glycerol molecule is assigned two dihedral angles, φ_1 and φ_2, which are formed by the three carbon atoms and the two terminal oxygen atoms. This results in six possible conformations of the glycerol molecule; $\alpha\alpha$, $\alpha\beta$, $\alpha\gamma$, $\beta\beta$, $\beta\gamma$, and $\gamma\gamma$.[35] Previous neutron diffraction studies combined with EPSR on pure glycerol[36] and a concentrated glycerol solution[37] have found that glycerol molecules are predominantly found in one conformation, the $\alpha\beta$ conformation (Figure 2 A,B). Interestingly, in the dilute glycerol solution studied here, glycerol molecules adopt a much wider distribution of conformations (Figure 2C), including $\alpha\alpha$, $\alpha\beta$, and $\alpha\gamma$ conformations. The water molecules that were used were produced using the simple point charge (SPC) model.[38] A three-dimensional computer model of the solution is constructed and equilibrated using relevant interaction potentials (see Figure 1 for molecule conformation and Tables 2 and 3 for atomic geometry).

dx.doi.org/10.1021/jp2093862 |J. Phys. Chem. B 2012, 116, 1633–1641

Table 2. Geometry for Intramolecular Bonds within the Glycerol and Water Molecules Used in the EPSR Simulations[a]

intramolecular bond	length (Å)
O−CG	1.45
O−H	0.97
OC−H	0.97
OC−CC	1.45
CG−CC	1.54
CG−HG	1.08
CC−HG	1.08
OW−HW	1.00

[a] The geometry used for the glycerol molecules was optimized using the free computational chemistry software Ghemical 2.98.[34] The water molecules have been produced using the SPC model.[52]

Table 3. Geometry for Intramolecular Angles in Glycerol and Water Molecules Used in the EPSR Simulations[a]

intramolecular bond	angle (deg)
CG−O−H	109.90
CC−OC−H	108.33
O−CG−CC	108.88
CC−CG−HG	110.17
O−CG−HG	109.51
HG−CG−HG	108.57
CG−CC−CG	111.20
OC−CC−CG	108.72
CG−CC−HG	109.61
OC−CC−HG	108.96
HW−OW−HW	109.47

[a] The geometry for the glycerol molecules has been optimized using the free computational chemistry software Ghemical 2.98.[34] The water molecules have been produced using the SPC model.[52]

The charges and Lennard-Jones constants are shown in Table 4. Periodic boundary conditions were imposed, and the Coulomb interactions are truncated by means of a derivative of the reaction field method,[39] and other interactions are truncated as described previously, using a radial cutoff of 12 Å in both cases.[33] Information from the diffraction data is then introduced as a constraint, whereby the difference between observed and calculated partial structure factors enters as a perturbation potential to drive the computer model (via Monte Carlo updates of atomic positions) toward agreement with the measured data. The perturbation is refined in successive iterations of the procedure until a satisfactory fit is obtained. In this way an ensemble of three-dimensional molecular configurations of the mixture is generated, which exhibits average structural correlations that are consistent with the diffraction data.

3. RESULTS

The total normalized structure factors $F(Q)$ for all five glycerol−water samples are shown in Figure 3 (black circles) together with the EPSR fits (red lines). The agreement between the experimental and fitted data is excellent. The experimental data and computational modeling output are labeled according to Table 1 and have been shifted vertically for improved clarity. Thus it is possible to conclude that the model that is produced using EPSR is physically plausible and reproduces the data available from the neutron diffraction experiment.

Table 4. Lennard-Jones Parameters, Masses, and Coulomb Charges Defining the Potentials Used for EPSR Simulations of Glycerol and Water at 298 K

atom name	ε (kJ/mol)	σ (Å)	m (a.m.u.)	q (e)
OC	0.65	3.100	16	−0.624
O	0.65	3.100	16	−0.624
CG	0.80	3.700	12	0.107
CC	0.80	3.700	12	0.170
H	0.00	0.000	2	0.392
HG	0.00	0.000	2	0.063
OW	0.65	3.166	16	−0.820
HW	0.00	0.000	2	0.410

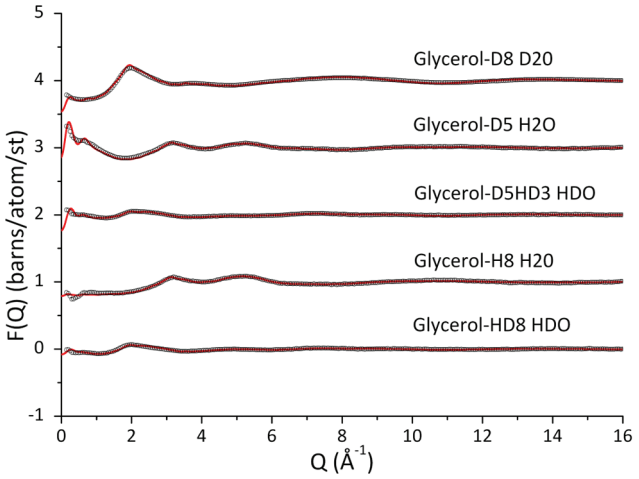

Figure 3. Diffraction pattern (black circles) and EPSR-fitted diffraction pattern (red line) for different isotope substitutions of a dilute glycerol water solution (0.05 mol fraction glycerol) at 298 K. The data and fits are labeled according to Table 1 and have been shifted vertically for improved clarity. The data shown here confirm that this model produces a simulation that is in good agreement with the experimental data.

3.1. Structure of Water in the Solution. In order to determine whether the structure of water is modified by the presence of glycerol in this dilute solution, we examine the water−water partial RDFs extracted from the EPSR analysis. The water oxygen−water oxygen RDF in dilute aqueous glycerol (0.05 m.f.) is shown in Figure 4 (full lines). This is compared with the function produced using previously published pure water data,[40] which was analyzed using EPSR and the potentials and geometry shown in Tables 2−4 (dashed lines). It can be seen that the position of the first peak in the water oxygen−water oxygen RDF $g_{OW\text{-}OW}(r)$ (Figure 4) is not affected to any great extent by the addition of glycerol at this concentration. However, the position of the second peak is considerably modified, shifting inward by 0.20 Å. This movement can be appreciated using the inset found in Figure 4 where the RDFs have been shifted vertically to aid clarity. The second peak position is of particular interest, as it is an indicator of the tetrahedrality of the water structure.[41] Previous studies on related systems have suggested that a compression of the second-neighbor water−water contact distance may be a structural feature of a hydrophobic driving

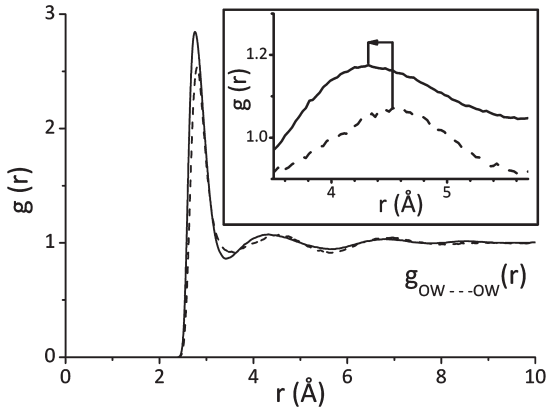

Figure 4. (A) Water oxygen−water oxygen site−site partial RDFs. The RDF is taken from the EPSR analysis of neutron diffraction data of a dilute glycerol−water (0.05 m.f.) mixture (solid lines) and are compared to results produced using previously published pure water data[40] (dashed lines). The second peak position is shown in the inset and shows a shift inward from 4.56 Å to 4.36 Å.

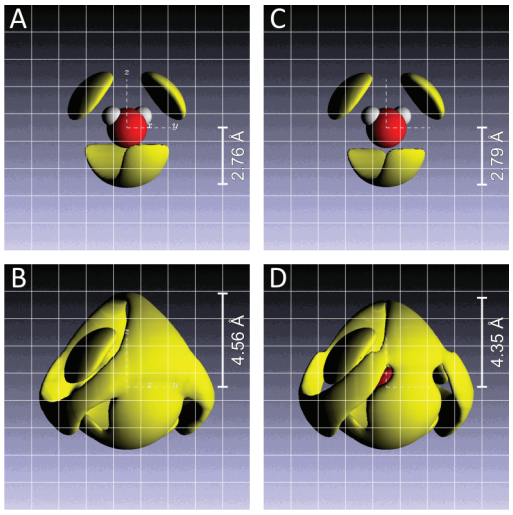

Figure 5. SDFs for the water oxygen atoms found around a central water molecule. The SDFs are taken from the EPSR analysis of neutron diffraction data taken from dilute (0.05 m.f.) glycerol−water samples (C,D) and are compared with the same functions for pure water (A,B). The yellow shaded areas represent the regions where the probability of finding another water molecule within 5.7 Å of the central oxygen atom exceeds 9% (top) and 20% (bottom). The average bond lengths are shown on the right-hand side of each of the images.

force.[42] In order to further investigate the three-dimensional structure of water in dilute glycerol spatial density functions (SDFs) have been calculated. The SDFs shown in Figure 5 are the three-dimensional analogues of the $g_{OW\text{-}OW}(r)$ RDF displayed in Figure 4. The SDF is produced by fixing the orientation of a central molecule and using this as the foundation for a coordinate system. The number of molecules that surround this central molecule are then calculated as a function of radial distance, azimuthal angle and elevation angle. This is then repeated for each of the relevant molecules in an ensemble of configurations. Figure 5 shows the SDFs for water molecules around a central water molecule. These SDFs are taken from the EPSR analysis of aqueous glycerol at a concentration of 0.05 m.f. (Figure 5 C,D). These are compared with SDFs produced using previously published pure water data,[40] which was analyzed using EPSR and the potentials and geometry shown in Tables 2−4 (Figure 5A,B). In the case of pure water (Figure 5A,B), the familiar tetrahedral first coordination shell can be seen, and a well-defined second shell then follows this (B). These features are repeated in the case of the water structure taken from the dilute aqueous glycerol result (Figure 5 C,D). There is, however, a slight inward shift in the position of the second shell. This shows that the addition of glycerol marginally shifts the second neighbor shell position within water inward.

Given the recurring hypothesis that glycerol acts to modify water structure, it is interesting to compare the structure of water in the dilute glycerol solution with the structure of water in the presence of other solutes at dilute concentrations, as well as to water under different temperature and pressure conditions. Previous X-ray scattering studies on pure water under pressure (5 kbar) found that the second peak of the water oxygen−water oxygen RDF $g_{OW\text{-}OW}(r)$ shifted inward by 0.18 Å.[43] A combined X-ray diffraction and ab initio molecular dynamics simulation study of pure water showed that as the temperature is reduced to 2 °C, the second peak of the RDF $g_{OW\text{-}OW}(r)$ became sharper and shifted inward by ~0.20 Å.[44] In agreement with both of these studies, a neutron diffraction study of pure water across a wide range of temperatures and pressures showed that the second peak of the RDF $g_{OW\text{-}OW}(r)$ shifted inward[40] with increasing pressure. Therefore the presence of small quantities of glycerol in the solution has the same effect on water structure as increasing the pressure and/or lowering the temperature of pure water. This is slightly surprising given the notion that cryoprotectant molecules act to reduce the ice-like nature of water. Instead, we find that the local water structure is becoming more like liquid water at low temperature. However, it is worth remembering that the freezing point of water decreases as the pressure increases.[45] Therefore, perhaps the action of glycerol is to drive water toward its structure at high pressure, at which point its freezing temperature reduces, thus protecting it from forming ice.

Next we consider the local water structure in other dilute aqueous solutions. Neutron diffraction studies of dilute aqueous methanol (0.05 m.f.) at room temperature measured a substantial inward shift of 0.3 Å in the second peak of the RDF $g_{OW\text{-}OW}(r)$.[42] An inward shift of 0.3 Å was also observed in dilute aqueous disaccharide trehalose (0.01 m.f.).[46] Conversely, neutron diffractions studies on dilute aqueous dimethyl sulphoxide (0.048) observed the second peak of the RDF $g_{OW\text{-}OW}(r)$ moved outward and flattened.[47] Neutron diffraction studies of dilute aqueous tertiary-butanol (0.06 m.f.) lead to an outward shift of the RDF $g_{OW\text{-}OW}(r)$.[48]Therefore, our observation of inward shift of the RDF $g_{OW\text{-}OW}(r)$ in dilute aqueous glycerol is an effect similar to that seen under pressure[43] and for dilute solutions of methanol[42] and trehalose,[46] while it differs from the effect seen in dilute solutions of dimethyl sulphoxide[47] and tertiary-butanol.[48] Interestingly, methanol,[50] trehalose,[51] and dimethyl sulphoxide[50] are all commonly used as cryoprotectants. This suggests that the cryoprotective action of these molecules may be different, as indeed is their impact on local water structure.[42−51]

3.2. Structure of glycerol in the solution. To further explore the liquid mixture, we next examine the structural properties of glycerol. We examine glycerol−glycerol pairwise distributions in the dilute solution and compare them with the same distributions in pure glycerol.[36] The three glycerol carbon-glycerol carbon RDFs ($g_{CG\text{-}CC}(r)$, $g_{CC-CC}(r)$, and $g_{CG\text{-}CG}(r)$) are displayed in

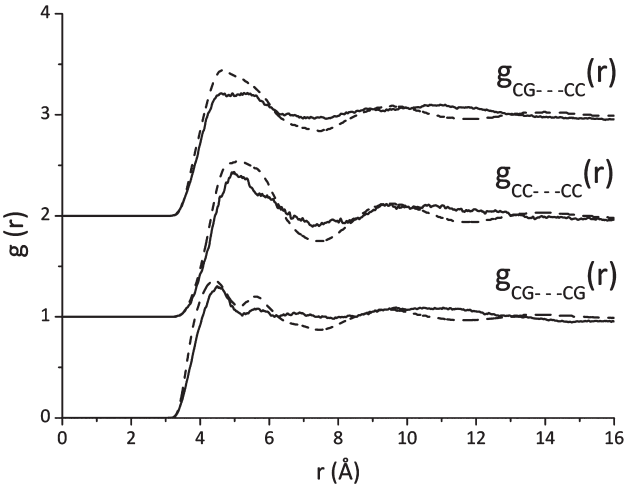

Figure 6. Glycerol−glycerol site−site partial RDFs for each of the three possible carbon−carbon pairings ($g_{CG\cdots CC}(r)$, $g_{CC\cdots CC}(r)$, and $g_{CG\cdots CG}(r)$) between the glycerol molecules. The RDFs are taken from the EPSR analysis of neutron diffraction data taken from dilute (0.05 m.f.) glycerol−water samples (solid lines) and are compared to results taken from pure glycerol data[36] (dashed lines). Here it can be seen that the first peak positions are not altered when glycerol is diluted by the addition of water. Interestingly, the longer-range order (>8 Å) is no longer present after dilution.

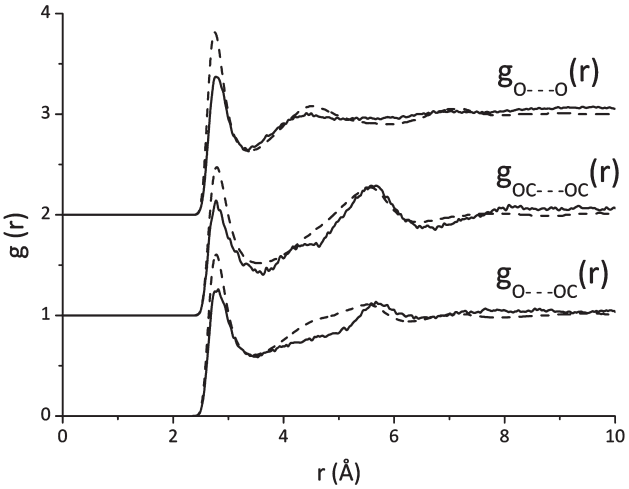

Figure 7. Glycerol−glycerol site−site partial RDFs for each of the three possible oxygen−oxygen pairings ($g_{O\cdots O}(r)$, $g_{OC\cdots OC}(r)$, and $g_{O\cdots OC}(r)$) between the glycerol molecules. The RDFs are taken from the EPSR analysis of neutron diffraction data taken from dilute (0.05 m.f.) glycerol−water samples (solid lines) and are compared to results from pure glycerol data[36] (dashed lines). Here it can be seen that the first peak positions are not altered when glycerol is diluted by the addition of water. Interestingly, the second peaks are greatly diminished within the $g_{O\cdots O}(r)$ and $g_{O\cdots OC}(r)$ functions after dilution. However, the second peak of the $g_{OC\cdots OC}(r)$ remains after mixing with water.

Figure 6, where the aqueous glycerol samples (full lines) are compared with previously published work on pure glycerol samples (dashed lines).[36] The first peak in the carbon−carbon RDFs (in Figure 6) are at a distance of 4.50−5.01 Å and are quite broad. It can be seen that the first peak positions for each of the RDFs is not modified to any great extent by the presence of water. Interestingly, the long-range structure found in pure glycerol[36] is greatly diminished. Again, it is interesting to compare the solute−solute interactions of glycerol with that of another dilute aqueous solution. A previous study of dilute aqueous methanol (0.05 m.f.) found a sharp peak in the $g_{C-C}(r)$ RDF at 4.09 Å.[42] This, combined with additional information, was used to show that the dominant methanol−methanol interaction is via the methyl groups, i.e., a hydrophobic interaction. The peaks seen within the carbon−carbon RDFs of glycerol (in Figure 6) are at a larger distance than that observed in methanol and are much broader than those found between methanol molecules. This suggests that the carbon−carbon interaction between glycerol molecules is less pronounced than that seen between methanol molecules. This interaction can be used as an indicator of hydrophobic interactions in a solution, suggesting that the hydrophobic interaction between glycerol molecules is not strong in this dilute solution. The structure of the hydroxyl portion of the glycerol molecules is shown in Figure 7. This shows the three glycerol oxygen−glycerol oxygen RDFs ($g_{O-O}(r)$, $g_{OC\text{-}OC}(r)$, and $g_{O\text{-}OC}(r)$). Again, the dilute (0.05 m.f.) aqueous glycerol samples (solid lines) are compared with previously published data on pure glycerol[36] (dashed lines). These show that the first peak positions for each of the RDFs shown are not greatly affected by the dilution in water (maximum shift in position is 0.03 Å. This shows that the structure of the hydroxyl portion of the glycerol molecules is not affected by dilution in water to the concentration studied here.

3.3. Glycerol and Water Hydrogen Bonding Ability. Given the local structure (first neighbor level) of water and glycerol are largely unperturbed from that found in the pure component, we next examine the overall hydrogen bond ability between the molecules. Previous studies have suggested that glycerol acts to diminish the hydrogen bond ability of water.[18] To shed light on this suggestion, we calculated the number of hydrogen bonds formed by water and by glycerol in the dilute solution, i.e., glycerol−glycerol, water−water, and glycerol−water. The relevant oxygen−hydrogen RDFs for each interaction are shown in Figure 8A. From this it can be seen that all of the RDFs have a first peak at around 1.8 Å (dashed line). This peak is characteristic of hydrogen bonding and shows that glycerol−glycerol, glycerol−water, water−glycerol, and water−water hydrogen bonds exist. The hydrogen bonding can be quantified by calculating the coordination number of hydrogen bonding between each glycerol and water hydroxyl group pair (see eq 4). The coordination numbers for hydrogen bonding between glycerol and water are shown in Table 5. In Figure 8B we show the hydrogen bonding ability of water and glycerol in the dilute glycerol solution and compare this with their ability in pure form. On average there are 3.4 ± 0.1 water−water hydrogen bonds per water molecule in the dilute glycerol sample. Water also forms an average of 0.3 ± 0.8 hydrogen bonds to glycerol molecules. This results in a total of 3.7 ± 1.3 hydrogen bonds per water molecule. By comparison, the number of hydrogen bonds per water molecule in pure water is 3.7 ± 0.9 (Tables 2−4). Therefore the number of water−glycerol hydrogen bonds compensates for the reduction in water−water hydrogen bonds, and there is no evidence for a diminished hydrogen bonding ability in water. Interestingly we also find that water molecules are equally likely to bind to the central or distal oxygen of the glycerol molecules. This is contradictory to previous studies[23] using Raman spectroscopy, which suggested that water molecules preferentially bond to the central oxygen of the glycerol molecule. Figure 4 also shows the number of hydrogen bonds formed by glycerol molecules in the dilute

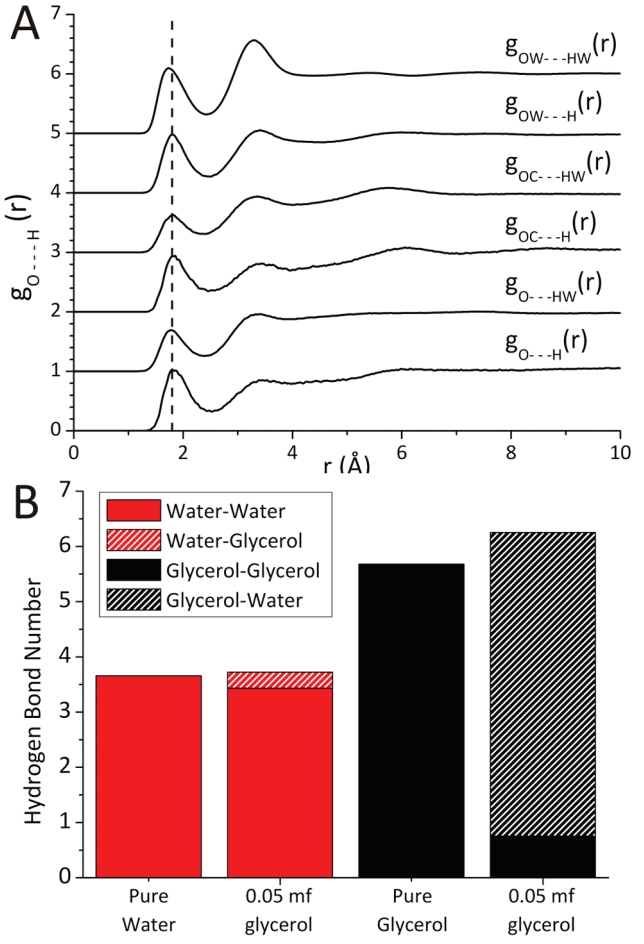

Figure 8. (A) Oxygen−hydrogen site−site partial RDFs for each of the possible oxygen−hydrogen pairings within the simulation. The RDFs are taken from the EPSR analysis of neutron diffraction data taken from dilute (0.05 m.f.) glycerol−water samples. Each of the 6 RDFs have a peak at around 1.8 Å (dashed line), characteristic of hydrogen bonding. (B) Using the data from the EPSR analysis of the neutron diffraction data, we calculate the number of hydrogen bonds per water molecule and per glycerol molecule in the dilute glycerol−water solution (0.05 m.f.) at 298 K. For comparison, we show the number of hydrogen bonds formed by both water and glycerol in the pure components, taken from previously published neutron diffraction studies on pure water[40] and pure glycerol.[36]

solution. In total, glycerol forms 6.3 ± 1.4 hydrogen bonds, as compared with 5.7 ± 1.5 hydrogen bonds in pure glycerol. This shows that glycerol molecules are more effective at forming hydrogen bonds in the presence of water, suggesting that the carbon backbone of glycerol molecules is more flexible or adaptable in the dilute solution, than in the pure glycerol liquid. This is in agreement with our analysis of the backbone conformations of glycerol (Figure 2) where a larger distribution of glycerol backbone conformations were found in the dilute solutions, as compared with pure glycerol. The conformational diversity of the glycerol molecule results in efficient hydrogen bonds with water molecules, resulting in a larger total number of hydrogen bonds. Therefore, while glycerol−glycerol hydrogen bonds are minimal (Figure 8B), glycerol efficiently hydrogen bonds with the surrounding water molecules. This suggests that glycerol molecules exist in isolation in this solution.

Table 5. Coordination Numbers Taken from the Relevant Oxygen−Hydrogen RDFs[a]

bond	r_{min} (Å)	r_{max} (Å)	coordination number	Σ
O−H	0.00	2.52	0.1	0.4
H−O	0.00	2.46	0.1	0.3
O−HW	0.00	2.40	1.1	0.7
HW−O	0.00	2.40	0.1	0.2
OC−H	0.00	2.49	0.1	0.4
H−OC	0.00	2.55	0.0	0.2
OC−HW	0.00	2.40	1.1	0.7
HW−OC	0.00	2.40	0.0	0.2
OW−H	0.00	2.46	0.1	0.3
H−OW	0.00	2.46	0.8	0.5
OW−HW	0.00	2.43	1.7	0.7
HW−OW	0.00	2.43	0.9	0.5

[a] The standard deviation (Σ) has been calculated over 806 configurations for each of the coordination numbers.

3.4. Hydrogen-Bonded Clusters. To further examine the location of glycerol molecules in the dilute solution, we calculate the cluster size distribution, which is the probability of finding a cluster of a particular size as a function of cluster size. The EPSR-generated ensembles were interrogated to extract structural information on glycerol clusters in the solution. The glycerol clusters are defined by those molecules that participate in a continuous hydrogen bonded network.[26] Two glycerol molecules are considered to be hydrogen-bonded if the interoxygen contact distance is less than the radial distance of the first minimum of the $g_{OO}(r)$ (Figure 7). Figure 9A shows the number of clusters containing i glycerol molecules as a fraction of the total number of clusters $M(i)/M$ [where $M = \Sigma_i M(i)$] against cluster size i. Here, the data extracted from the EPSR simulation (squares) is compared to that taken from a simulation where the Coulombic and empirical potentials have been removed (triangles). The simulation was run at the same glycerol concentration with the same intramolecular bond lengths and angles (Tables 2 and 3) but with no atomic charges and the empirical potential set to zero, thus removing all of the attractive interactions between the molecules other than van der Waals interactions. Any clustering/segregation found in the results taken from the simulation without Coulombic or empirical potentials can be ascribed to molecular packing. Figure 9B shows that many glycerol molecules (40%) exist as monomers in a dilute glycerol−water (0.05 m.f. glycerol) mixture (squares), while a small number of large clusters exist. The largest clusters were found to consist of 32 glycerol molecules. The cluster size distribution for the system where Coulombic and empirical potentials have been removed (triangles) shows that only 9% of the glycerol molecules exist as monomers in the solution, with the majority of glycerol molecules existing in clusters of size two or more, with a maximum cluster size of 168 glycerol molecules (Figure 9A). This shows that the monomers shown within the EPSR simulation are not simply due to a packing effect. The lack of glycerol clustering suggests that water−glycerol interactions are more favorable than water−water interactions, at this concentration. This results in a solution that has a large number of isolated glycerol molecules that are bonded to the surrounding water molecules. A representative snapshot of the dilute glycerol water solution is shown in Figure 9C (upper) where water molecules

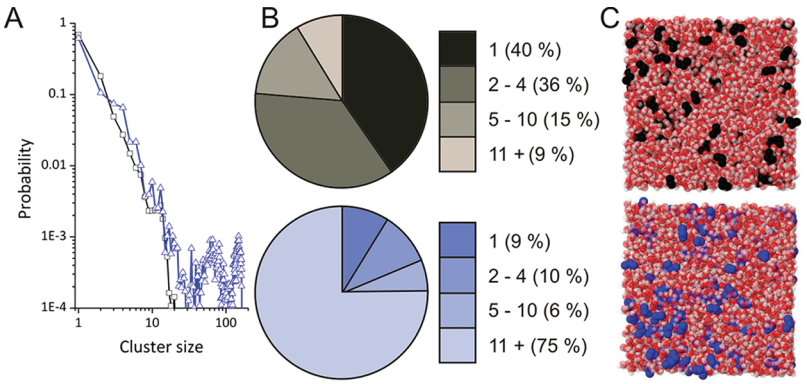

Figure 9. Glycerol−glycerol molecule cluster size distribution in a dilute glycerol water solution (0.05 m.f.). Cluster size distributions are shown for EPSR analysis of neutron diffraction data (squares) and a simulation where glycerol and water molecules are randomly packed (all Coulombic and empirical potentials have been omitted) (triangles). A glycerol molecule is defined as being in the same cluster as another if any of the three oxygen atoms are within a specified distance of the oxygen atoms on another glycerol molecule. The specified distance is taken from the position of the relevant trough within the glycerol oxygen−oxygen RDFs. The EPSR cluster distribution (squares) shows a maximum cluster size of 32 molecules, while the random packing simulation shows a maximum cluster size of 168 glycerol molecules. (B) Pie chart showing the proportion of glycerol molecules that are found within clusters of different sizes in a dilute glycerol−water solution (0.05 m.f.) from the EPSR simulation (upper) and in the random packing simulation (lower). In the pie charts, monomers (clusters size of one) are shown with the darkest colors, and lighter shades are used for clusters with increasing size. (C) Representative snapshots from the EPSR simulation of the dilute glycerol−water solution (upper) and from the random packing simulation (lower), where water molecules are represented by their oxygen atoms (red spheres) and hydrogen atoms (gray spheres) and glycerol molecules are represented by their carbon atoms in the backbone (black spheres for the ESPR simulation and blue spheres for the random molecular packing simulation). The snapshots demonstrate that in the EPSR simulation many glycerol molecules exist as isolated molecules, efficiently hydrogen bonding with the surrounding water molecules.

are represented by their oxygen atoms (red) and hydrogen atoms (gray spheres), and glycerol molecules are represented by their carbon atoms in the backbone (black spheres). The snapshot demonstrates that many glycerol molecules exist as isolated molecules, efficiently hydrogen bonding with the surrounding water molecules. This picture is striking when compared with a representative snapshot from the random packing simulation (Coulombic and empirical potentials removed) where glycerol molecules form much larger clusters and very few monomer are present (Figure 9C, lower).

4. DISCUSSION

In this study we have examined the hydrogen bonding of glycerol and water in a dilute mixture (0.05 m.f. glycerol). This has been achieved by a combination of neutron diffraction with isotopic substitution and EPSR modeling. The models that have been produced for glycerol and water are consistent with the experimental results and provide new insight into the structural properties of an important cryoprotectant molecule. Given the hypothesis that glycerol acts to modify the structure of water, it is interesting that no change to the local structure of water is found, at least at the first water−water neighbor level. A small inward shift of the second coordination shell of water is observed, as has previously been observed for water under pressure, and in the presence of methanol and trehalose. This observation suggests that cryoprotectants such as glycerol, methanol, and trehalose may act to modify water structure beyond the first neighbor level. This may have an impact on the extended hydrogen bond network that water forms, and consequently the ability of water to form ice at low temperatures. Interestingly, we find that water adopts a structure that is similar to that of pure water at high pressure. Given water under pressure freezes at a lower temperature, our studies suggest that glycerol molecules act to "pressurize" water and thus lower its freezing temperature—an effective cryoprotective mechanism for inhibiting ice formation. Indeed, it is noteworthy that the freezing temperature of a dilute glycerol water solution (0.05 m.f.) is −5.3 °C.

Given glycerol's role as a cryoprotectant molecule, it is interesting to compare the structural properties of glycerol, a sugar alcohol, with that of methanol, an alcohol. A cluster analysis of the distribution of glycerol molecules (Figure 9A), derived from the EPSR simulation of the experimental data, provides structural insight into glycerol clusters in the solution. Previous work has shown that methanol−water mixtures microsegregate to form water-rich and methanol-rich clusters.[26,27,42] This work showed that in a dilute methanol−water (0.05 m.f.) mixture, methanol molecules exist as clusters in a fluid of close-packed methyl groups, with water clusters bridging neighboring methanol hydroxyl groups through hydrogen bonding. Furthermore, although single methanol molecules exist (cluster size 1), these constitute only 20% of all methanol molecules in the mixture. The remaining 80% methanol molecules occur in clusters containing two to eight or more molecules. Conversely, in the dilute glycerol−water (0.05 m.f.) mixture in the present study, we find that many glycerol molecules exist as isolated monomers (40%). This preference for isolated glycerol molecules is more than just a simple packing effect where we might expect around 9% of isolated water molecules. Furthermore, while in the EPSR simulation we find a largest glycerol cluster size of 32 glycerol molecules, in the case of a randomly packed solution, the largest cluster size is much larger (168 molecules). Therefore, in a dilute glycerol−water solution there seems to be a preference for isolated glycerol molecules that goes beyond that expected for the mixture. Given the presence of unperturbed water−water interactions and the lack of large glycerol clusters, it is interesting to consider the role played by glycerol in preventing ice formation. We find that glycerol and water molecules mix very effectively, hindering the formation of an extended glycerol and water network in the solution. Indeed, the number of water−glycerol hydrogen bonds

has been shown to compensate for the reduction in water−water and glycerol−glycerol hydrogen bonding. This result is consistent with the findings of the molecular dynamics simulations of Politi et al.[24] and Dashnau et al.,[19] which found that water−glycerol hydrogen bonds compensate for the loss of water−water bonds on dilution. Thus, the results of the neutron diffraction study reported here, along with previous studies,[19,24] cast doubt on the result of Chen et al.[18] who stated that the addition of glycerol reduced the ability of water to form hydrogen bonds. Furthermore, given the efficiency of glycerol molecules to take the place of water molecules in the hydrogen bonded network, an extended water network is impeded. Thus, we propose that it is the good mixing of this solution and the preference of glycerol monomers that prevent glycerol and water networks from penetrating and perhaps disrupting biological systems. Given glycerol can be found in dilute concentrations in biological systems,[6] the mixing of aqueous glycerol and preference for glycerol monomers could offer an attractive structural mechanism for protecting organisms under extreme cold conditions. Further studies on the intermediate concentration of glycerol solutions will help to elucidate whether this structural picture is valid across the concentration regime.

■ ACKNOWLEDGMENT

This work was supported by the Engineering Physical Science Research Council, U.K. through Grant EP/H020616 to L.D. and through a DTA studentship to J.J.T. Experiments at the ISIS Pulsed Neutron and Muon Source were supported by a beam time allocation from the Science and Technology Facilities Council. We are grateful to Prof. Alan Soper, Dr. Silvia Imberti, and Dr. Rowan Hargreaves at the ISIS Facility, Rutherford Appleton Laboratory, for their support. We thank Prof. Stephen Evans and Dr. Kasia Tych for useful discussions and Natasha Rhys for critical reading of the manuscript.

■ REFERENCES

(1) Cook, R. L.; King, H. E.; Herbst, C. A.; Herschbach, D. R. *J. Chem. Phys.* **1994**, *100*, 5178.
(2) Davies, D. B.; Matheson, A. J.; Glover, G. M. *J. Chem. Soc., Faraday Trans. 2* **1973**, 305.
(3) Champeney, D. C.; Kaddour, F. O. *Mol. Phys.* **1984**, *52*, 509.
(4) Menon, N.; Nagel, S. R. *Phys. Rev. Lett.* **1995**, *74*, 1230.
(5) Bohmer, R.; Hinze, G. *J. Chem. Phys.* **1998**, *109*, 241.
(6) Benamotz, A.; Avron, M. *Plant Physiol.* **1973**, *51*, 875.
(7) Gekko, K.; Timasheff, S. N. *Biochemistry* **1981**, *20*, 4667.
(8) Raymond, J. A. *J. Exp. Zool.* **1992**, *262*, 347.
(9) Bernemann, I.; Hofmann, N.; Spindler, R.; Szentivanyi, A.; Glasmacher, B. *Cryoletters* **2008**, *29*, 83.
(10) Yancey, P. H.; Clark, M. E.; Hand, S. C.; Bowlus, R. D.; Somero, G. N. *Science* **1982**, *217*, 1214.
(11) Mazur, P. *Science* **1970**, *168*, 939.
(12) Salt, R. W. *Nature* **1958**, *181*, 1281.
(13) Garcia-Manyes, S.; Dougan, L.; Fernandez, J. M. *Proc. Natl. Acad. Sci. U.S.A.* **2009**, *106*, 10540.
(14) Doss, A.; Paluch, M.; Sillescu, H.; Hinze, G. *J. Chem. Phys.* **2002**, *117*, 6582.
(15) Kyrychenko, A.; Dyubko, T. S. *Biophys. Chem.* **2008**, *136*, 23.
(16) Bastiansen, O. *Acta Chem. Scand.* **1949**, *3*, 415.
(17) Callam, C. S.; Singer, S. J.; Lowary, T. L.; Hadad, C. M. *J. Am. Chem. Soc.* **2001**, *123*, 11743.
(18) Chen, C.; Li, W. Z.; Song, Y. C.; Yang, J. *J. Mol. Liq.* **2009**, *146*, 23.
(19) Dashnau, J. L.; Nucci, N. V.; Sharp, K. A.; Vanderkooi, J. M. *J. Phys. Chem. B* **2006**, *110*, 13670.
(20) To, E. C. H.; Davies, J. V.; Tucker, M.; Westh, P.; Trandum, C.; Suh, K. S. H.; Koga, Y. *J. Solution Chem.* **1999**, *28*, 1137.
(21) Doss, A.; Paluch, M.; Sillescu, H.; Hinze, G. *Phys. Rev. Lett.* **2002**, *88*, 095701.
(22) Vanderkooi, J. M.; Dashnau, J. L.; Zelent, B. *Biochim. Biophys. Acta, Proteins Proteomics* **2005**, *1749*, 214.
(23) Mudalige, A.; Pemberton, J. E. *Vib. Spectrosc.* **2007**, *45*, 27.
(24) Politi, R.; Sapir, L.; Harries, D. *J. Phys. Chem. A* **2009**, *113*, 7548.
(25) Pielak, G. J.; Batchelor, J. D.; Olteanu, A.; Tripathy, A. *J. Am. Chem. Soc.* **2004**, *126*, 1958.
(26) Dougan, L.; Bates, S. P.; Hargreaves, R.; Fox, J. P.; Crain, J.; Finney, J. L.; Reat, V.; Soper, A. K. *J. Chem. Phys.* **2004**, *121*, 6456.
(27) Dougan, L.; Hargreaves, R.; Bates, S. P.; Finney, J. L.; Reat, V.; Soper, A. K.; Crain, J. *J. Chem. Phys.* **2005**, *122*, 174514.
(28) Soper, A. K.; Dougan, L.; Crain, J.; Finney, J. L. *J. Phys. Chem. B* **2006**, *110*, 3472.
(29) Fischer, H. E.; Barnes, A. C.; Salmon, P. S. *Rep. Prog. Phys.* **2006**, *69*, 233.
(30) Soper, A. K.; Howells, S.; Hannon, A. C. *ATLAS - Analysis of Time-of-Flight Diffraction Data from Liquid and Amorphous Samples; RAL* Report RAL-89-046; 1989.
(31) Soper, A. K. *Mol. Phys.* **2009**, *107*, 1667.
(32) Soper, A. K. *Phys Rev B* **2005**, *72*, 104204.
(33) Soper, A. K. *Chem. Phys.* **1996**, *202*, 295.
(34) Hassinen, T.; Perakyla, M. *J. Comput. Chem.* **2001**, *22*, 1229.
(35) Bastiansen, O. *Acta Chem. Scand.* **1949**, *3*, 415.
(36) Towey, J. J.; Soper, A. K.; Dougan, L. *Phys. Chem. Chem. Phys.* **2011**, *13*, 9397.
(37) Towey, J. J.; Soper, A. K.; Dougan, L. *J. Phys. Chem. B* **2011**, *115*, 7799.
(38) Berendsen, H. J. C.; Grigera, J. R.; Straatsma, T. P. *J. Phys. Chem.* **1987**, *91*, 6269.
(39) Hummer, G.; Soumpasis, D. M.; Neumann, M. *J Phys-: Condens. Matter* **1994**, *6*, A141.
(40) Soper, A. K. *Chem. Phys.* **2000**, *258*, 121.
(41) Head-Gordon, T.; Johnson, M. E. *Proc. Natl. Acad. Sci. U.S.A.* **2006**, *103*, 7973.
(42) Dixit, S.; Soper, A. K.; Finney, J. L.; Crain, J. *Europhys. Lett.* **2002**, *59*, 377.
(43) Okhulkov, A. V.; Demianets, Y. N.; Gorbaty, Y. E. *J. Chem. Phys.* **1994**, *100*, 1578.
(44) Hura, G.; Russo, D.; Glaeser, R. M.; Head-Gordon, T.; Krack, M.; Parrinello, M. *Phys. Chem. Chem. Phys.* **2003**, *5*, 1981.
(45) *Handbook of Chemistry and Physics*, 91st ed.; Haynes, W. M., Ed; CRC Press: Boca Raton, FL, 2010.
(46) Pagnotta, S. E.; Ricci, M. A.; Bruni, F.; McLain, S.; Magazu, S. *Chem. Phys.* **2008**, *345*, 159.
(47) McLain, S. E.; Soper, A. K.; Luzar, A. *J. Chem. Phys.* **2007**, *127*, 174515.
(48) Bowron, D. T.; Finney, J. L.; Soper, A. K. *J. Phys. Chem. B* **1998**, *102*, 3551.
(49) Soper, A. K.; Castner, E. W.; Luzar, A. *Biophys. Chem.* **2003**, *105*, 649.
(50) Horvath, A.; Wayman, W. R.; Urbanyi, B.; Ware, K. M.; Dean, J. C.; Tiersch, T. R. *Aquaculture* **2005**, *247*, 243.
(51) Porto, L. C.; Rodrigues, J. P.; Paraguassu-Braga, F. H.; Carvalho, L.; Abdelhay, E.; Bouzas, L. F. *Cryobiology* **2008**, *56*, 144.
(52) Robinson, G. W.; Zhu, S. B.; Singh, S.; Evans, M. W. *Water in Biology, Chemistry and Physics: Experimental Overviews and Computational Methodologies*; World Scientific: Singaore, 1996.